Hawaii International Conference on System Sciences, January 2002, Hawaii.

Examining criticality of blackouts in power system models with cascading events

I. Dobson
ECE Department
Univ. of Wisconsin
Madison WI 53706
dobson@engr.wisc.edu

J. Chen J.S. Thorp
School of ECE
Cornell University
Ithaca NY 14850
thorp@ee.cornell.edu

B.A. Carreras
Oak Ridge National Laboratory
Oak Ridge TN 37831
carrerasba@ornl.gov

D. E. Newman
Physics Dept.
Univ. of Alaska
Fairbanks AK 99775
ffden@uaf.edu

Abstract

As power system loading increases, larger blackouts due to cascading outages become more likely. We investigate a critical loading at which the average size of blackouts increases sharply to examine whether the probability distribution of blackout sizes shows the power tails observed in real blackout data. Three different models are used, including two simulations of cascading outages in electric power transmission systems. We also derive and use a new, analytically solvable model of probabilistic cascading failure which represents the progressive system weakening as the cascade proceeds.

1. Introduction

Analyses [5, 8] of 15 years of North American blackout data [1] show a probability distribution of blackout size which has heavy tails and evidence of power law dependence in these tails [5, 8]. These analyses show that large blackouts are much more likely than might be expected from, say, a Gaussian distribution of blackout size in which the tails decay exponentially. The power tails of probability distributions of blackout size merit attention because of the enormous cost to society of large blackouts.

In complex systems, power tails in probability distributions are associated with systems at criticality. Other indicators of criticality are changes in gradient or a discontinuity in some measured quantity. One purpose of this paper is to examine the occurrence of power tails and criticality as power system loading is varied. We examine expected blackout size and pdfs as loading is varied in three different models. The first model is a simple analytic model of cascading failure and the second and third models are simulations of cascading outages in electric power transmission systems. In any power system, at zero loading there are no blackouts and at any absurdly large loading there is always a blackout. We examine the nature of the transition between these two extremes.

2. CASCADE model

We want to capture some general features of probabilistic cascading failure in a new model simple enough to allow exact analysis. The general features are:

1. Multiple components, each of which has a random initial loading.
2. When a component overloads, it fails and transfers some load to the other components.

Property 2 can cause cascading failure: an overload additionally loads other components and some of these other components may also overload, leading to a possible cascade of overloads. The extent of the cascade depends on the random initial component loadings. The components which are not (yet) overloaded become progressively more loaded as the cascade proceeds. Thus CASCADE models the weakening of the system as the cascade proceeds.

2.1. Description of model

The CASCADE model has n identical transmission lines with initial loadings (power flows) which are random. For each line the minimum loading is L^{min} and the maximum loading is 1. For j=1,2,...,n, line j has initial loading L_j which is a random variable uniformly distributed on $[L^{min}, 1]$. The average loading $L = (L^{min} + 1)/2$. Also $L^{min} = 2L - 1$. $L_1, L_2, \cdots, L_n$ are independent.

Lines are outaged when their loading exceeds 1. When a line is outaged, a fixed amount of load Δ is transferred to each of the lines. Thus Δ is the amount of load increase on any line when another line outages. Let p be the probability that L_1 lies in an interval of length Δ contained in $[L^{min}, 1]$:

$$p = \frac{\Delta}{1 - L^{min}} = \frac{\Delta}{2 - 2L} \qquad (1)$$

It is convenient to assume that the values of Δ are quantized so that $q = 1/p = (1 - L^{min})/\Delta$ is an integer. Then $[L^{min}, 1]$ can be partitioned into q intervals of length Δ.

To start the cascade, we assume an initial disturbance which loads each line by an additional amount Δ. Other lines may then outage depending on their loadings L_j and the outage of any of these lines will distribute an additional loading Δ that can cause further outages in a cascade.

The model parameters are summarized in Table 1. All the model parameters can be specified in terms of the average line loading L, the amount of load Δ distributed to each line upon an overload, and the number of lines n.

Table 1. CASCADE parameters

	description	comment
n	number of lines	
L	average line loading	
1	max line loading	
L^{min}	min line loading	$L^{min} = 2L - 1$
Δ	load increase at each line when outage	
p	probability L_1 in interval of length Δ	$p = \Delta/(2 - 2L)$
q	the integer $1/p$	$q\Delta = 1 - L^{min}$

2.2. Discussion of model

It is plausible that the general features of cascading failure captured in CASCADE can be present in cascading failure of power system transmission lines. However, CASCADE is much too simple to represent with realism most of the detailed and probably significant aspects of a power system. Obvious deficiencies of CASCADE include the transfer of loading upon overload without regard to network structure, an artificial uniformity in the transmission lines and their interactions, and no representation of generation changes or failure. Analysis of CASCADE can only suggest general qualitative behavior that may be present in power system cascading failures.

We discuss the parameter Δ. In a power system, suppose that a transmission line has maximum loading 1 and it overloads by a small amount so that the loading just before outage is approximately 1. Then, assuming a DC load flow model, the outage causes the other line flows to change according to line outage distribution factors [12]. The parameter Δ in CASCADE corresponds to line outage distribution factors averaged over all lines and all outaged lines. In practice, the line outage distribution factors vary considerably according to the lines considered. Only a subset of lines may have loading significantly increased or decreased by an outage.

If Δ is very roughly estimated by averaging line outage distribution factors, then it depends on the average amount of parallel paths in the network. In the special case of a network of all parallel lines, the amount of load transferred to other lines is $1/(\text{number of intact lines} - 1) \approx 1/n$, at least for the first few outages. In the case of the 179 bus model of the WSCC system with number of lines $n = 204$, the average line outage distribution factor is $0.0026 \approx 1/(2n)$. More highly meshed networks such as those in the Midwestern United States would tend to have smaller average line outage distribution factors.

In some cascading failures, power is redispatched so that an overload on a line is relieved. This also transfers power to other lines, but much less power is transferred than when the line outages. This process corresponds to a smaller value of Δ. There are also many other ways in which a disturbance can outage lines, including interactions via dynamics and via the protection system.

The overload of a line by redistribution of the power flow when another line outages depends both on the line loading and the line outage distribution factor. The CASCADE model has a fixed Δ corresponding to the line outage distribution factor but represents random variation in the line loadings.

2.3. Distribution of blackout size

Measure blackout size by S, the number of lines outaged. S is a discrete random variable on $0, 1, 2, ..., n$. The distribution of S is derived in appendix A and is given by the following formulas:

If $np \leq 1$ then

$$P[S = r] = \frac{1}{r+1} \binom{n}{r} ((r+1)p)^r (1 - (r+1)p)^{n-r} \tag{2}$$

If $np \geq 1$, then $q = 1/p \leq n$ and

$$P[S = r] = \begin{cases} \text{equation (2)} & ; r \leq q - 1 \\ 0 & ; q \leq r \leq n - 1 \\ 1 - \sum_{s=0}^{n-1} P[S = s] & ; r = n \end{cases} \tag{3}$$

Note that (2) gives $P[S = q - 1] = 0$ and that (2) and (3) agree for $np = 1$.

Consul [9] introduced the following quasibinomial distribution to model an urn problem in which the player makes strategic decisions:

$$P[X = r] = \binom{n}{r} p(p + r\phi)^{r-1}(1 - p - r\phi)^{n-r} \tag{4}$$

for $r = 0, 1, ..., n$ and $p + n\phi \leq 1$. For the special case $\phi = p$ and $(n + 1)p \leq 1$, we have $X = S$ and that S has the quasibinomial distribution. Consul [9] has derived the mean of distribution (4) and by setting $\phi = p$ in Consul's formula, we obtain

$$ES = np \sum_{r=0}^{n-1} \frac{(n-1)!}{(n-r-1)!} p^r \qquad , np \leq 1 \tag{5}$$

2.4. Results

The distribution of blackout size S defined by (2), (3) depends on p and n. For the first series of results we use 100 lines ($n = 100$). The mean blackout size ES as a function of p is shown in Figure 1. There is a change in slope near $p = 0.01 = 1/100$ and, for larger p, the mean blackout size saturates at 100 lines.

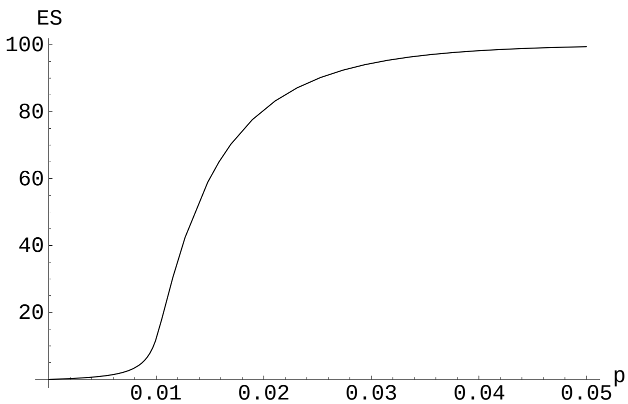

Figure 1. Mean blackout size ES versus probability p for $n = 100$.

Choose $\Delta = 0.005 = 1/(2n)$. Then the mean blackout size ES as a function of average loading L is shown by the solid line in Figure 2. For a fixed Δ, Figure 2 is obtained from Figure 1 by changing the horizontal axis quantity according to $L = 1 - \Delta/(2p)$. For $\Delta = 0.005$, the change in slope in Figure 2 corresponds to p near 0.01 and occurs near loading $L = 1 - 0.005/0.02 = 0.75$.

In the CASCADE model we can roughly approximate the mean power served as proportional to the average line loading and to the average number of intact lines:

$$\text{mean power served} \propto L(n - ES) \tag{6}$$

Mean power served is plotted in Figure 2. The maximum mean power served occurs at the critical loading as a consequence of the sharp rise in ES becoming dominant in (6).

Figure 3 shows the distribution of S for $p = 0.005$ on a log-log plot. The distribution of S falls off for larger blackouts in a more exponential fashion and the probability of most or all of the lines blacking out is negligible.

Figure 4 shows the distribution of S when p is increased to the critical value of $p = 1/n = 0.01$. There is a heavy tail

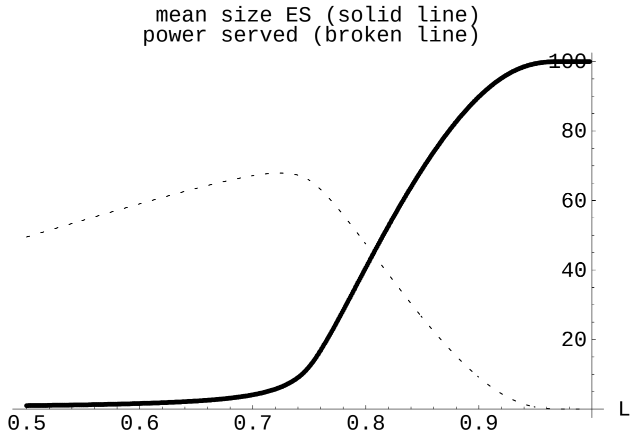

Figure 2. Mean blackout size ES and mean power served versus loading L. Power served has arbitrary units and $n = 100$.

in the distribution in which there is non-negligible probability of most or all of the lines blacking out. The distribution of S over an initial range of say, 0 to 25, is close to, but not exactly a power law. The region of behavior close to a power law is maximized for $p \approx 1/n = 0.01$.

Figure 5 shows the distribution of S when p is further increased to $p = 0.015$. The probability of the entire network blacking out is 0.60. There is also significant probability of short cascades and the distribution of these short cascades falls off in a more exponential fashion.

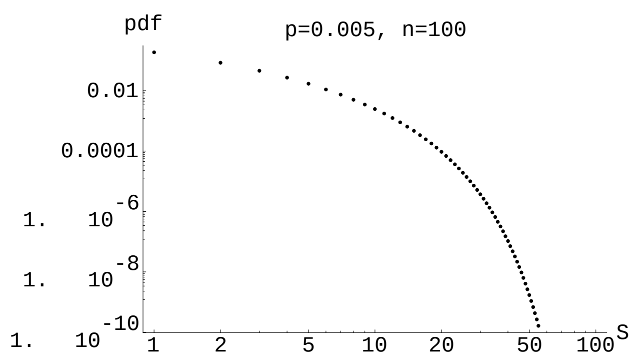

Figure 3. PDF of blackout size S. (P[S=0]=0.61 is not plotted.)

Now we briefly examine the scaling of the critical change in slope in Figure 1 with the number of lines n. It is useful to express the mean blackout size as the mean fraction of lines failed and to examine the mean blackout size as a function of the scaled probability np. Figure 6 shows the slope change for $n = 20, 100, 500$. The change in slope

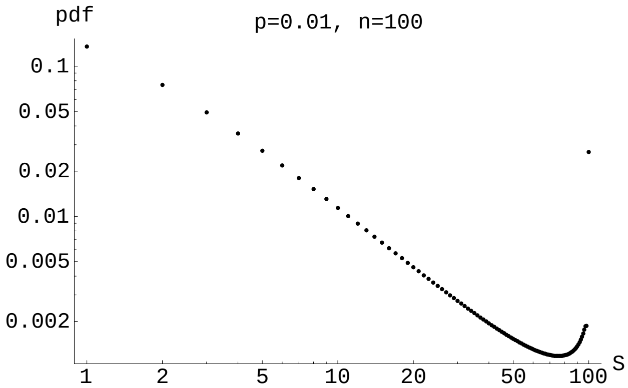

Figure 4. PDF of blackout size S. (P[S=0]=0.37 is not plotted.)

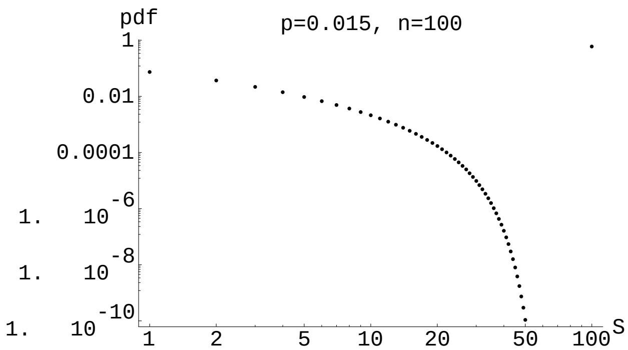

Figure 5. PDF of blackout size S. (P[S=0]=0.22 not plotted; note P[S=100]=0.60)

in Figure 6 occurs at $np = 1$ and becomes sharper as n increases. The slopes of the curves in Figure 6 peak at $np = 1$. These features of Figure 6 suggest a type 2 phase transition at $np = 1$. There is also a change in regime from formula (2) to formula (3) when $np = 1$.

We can analytically approximate the pdf of blackout size. Using Stirling's formula $m! \approx \sqrt{2\pi m}\,(m/e)^m$ to approximate the factor $n!/((r+1)!(n-r)!)$ in (2),

$$P[S = r] \approx \frac{e}{\sqrt{2\pi}} \sqrt{\frac{n}{n-r}} \frac{(np)^r}{(r+1)^{3/2}} \left(1 + \frac{r - (r+1)np}{n-r}\right)^{n-r} \quad (7)$$

and, for large enough $n-r$, using $(1+y/(n-r))^{(n-r)} \approx e^y$ and $\sqrt{1 - r/n} \approx 1$, we get

$$P[S = r] \approx \frac{(np)^r e^{(1-np)(r+1)}}{\sqrt{2\pi}\,(r+1)^{3/2}} \quad (8)$$

In approximation (8), the distribution of S depends only on

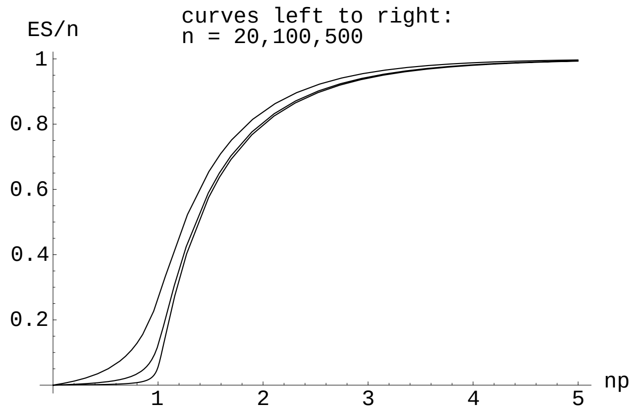

Figure 6. Fractional mean blackout size ES/n versus scaled probability np.

np. Moreover, if $np = 1$, then

$$P[S = r] \approx \frac{1}{\sqrt{2\pi}\,(r+1)^{3/2}} \quad (9)$$

and (9) predicts that the slope in Figure 4 is ≈ -1.5. The actual slope in Figure 4 varies between -1.0 and -1.3 for $2 \leq S \leq 45$ and is ≈ -1.3 for $6 \leq S \leq 28$. For np not close to 1, the expression $(np\, e^{(1-np)})^r$ in (8) will cause the distribution to decrease more exponentially for $r << n$.

The increased prevalence of large blackouts near critical loading can be attributed to the progressive loading and weakening of the network as lines outage. If one removes the progressive loading so that there is no increase of load when lines outage ($\Delta = 0$), but retain the initial disturbance of Δ, then the distribution of blackout sizes becomes binomial:

$$P[S = r] = \binom{n}{r} p^r (1-p)^{n-r} \quad (10)$$

3. Hidden Failure Model

When a transmission line trips, there is a small but significant probability that lines connected to either end of the tripped transmission line may incorrectly trip due to relay misoperation. These further line trippings are called hidden failures because they do not become apparent until the first line tripping "exposes" the adjacent lines to the possibility of relay misoperation. Recent NERC reports [1] show that hidden failures in protection systems have played a significant role in cascading disturbances. In this section, we summarize the hidden failure model presented in [8] and show simulation results about how the blackouts depend on system loading.

The hidden failure model uses the DC load flow approximation, in which the linearized, lossless power system is equivalent to a resistive circuit with current sources. In particular, transmission lines may be regarded as resistors and generation and load may be regarded as current sources and sinks. The probability of an exposed line tripping incorrectly is modeled as a increasing function of the line flow seen by the line relay. The probability is low below the line limit, and increases linearly to 1 when the line flow is 1.4 times the line limit.

The simulation begins by randomly choosing an initial line trip. This action exposes all lines connected to the ends of the initial line and also may overload lines. If one line flow exceeds its preset limit then the line is tripped. Otherwise, a line protection hidden failure mechanism [2, 11] is applied to let the chosen exposed line trip. After each line trip, the line flows are recalculated and checked for violations in line limits. The process is repeated until the cascading event stops.

As a final step, an optimal distribution of generation and load is calculated. Linear programming is used to minimize the amount of load shed subject to the constraints of the generation and load lying within their upper and lower limits, the line flows not exceeding the maximum flow, and overall generation matching the overall load.

The above simulation is repeated over an ensemble of randomly selected transmission lines as the initiating fault location.

We discuss an improvement of the hidden failure model. Suppose that a line is exposed multiple times by trippings of multiple lines connected to it. One would expect that, if relay misoperation occurs, it will occur on the first exposure of the line and is unlikely to occur on the subsequent exposures. However, the previous version of the model in [8, 2, 11] allowed relay misoperation with equal probability on all the line exposures. The improved model reduces or zeros the probability of misoperation after the first exposure.

We simulate a WSCC equivalent system with 179 buses, 29 generators, 60 transformers, and 203 transmission lines. The initial load flow data is based on the December 12, 1994 conditions, from which the required DC load flow data is derived.

NERC reports [1] show that there are only about 150 events during the past 16 years in the WSCC region. A direct simulation of these rare events would require an unrealistically huge amount of computation. One way out of this quandary is to use importance sampling [3]. In importance sampling, rather than using the actual probabilities, the simulation uses altered probabilities so that the rare events occur more frequently. Associated with each distinct sample path, SP_i, a ratio of actual probability of the event p_i^{actual} divided by the altered probability $p_i^{simulate}$ is computed. We then form the estimated probability of SP_i as

$$\hat{\rho}_i = \frac{N_{occurring}}{N_{total}} \cdot \frac{p_i^{actual}}{p_i^{simulate}} \tag{11}$$

where $N_{occurring}$ is the number of times that SP_i occurred and N_{total} is the total number of samples. The mean value of $\hat{\rho}_i$ is unbiased [3]. The power loss P_i associated with each sample path is also recorded.

Figure 7 shows the expected power loss

$$EP = \sum P_i \, \hat{\rho}_i \tag{12}$$

as a function of loading level L. The change in slope occurs near loading $L = 0.75$.

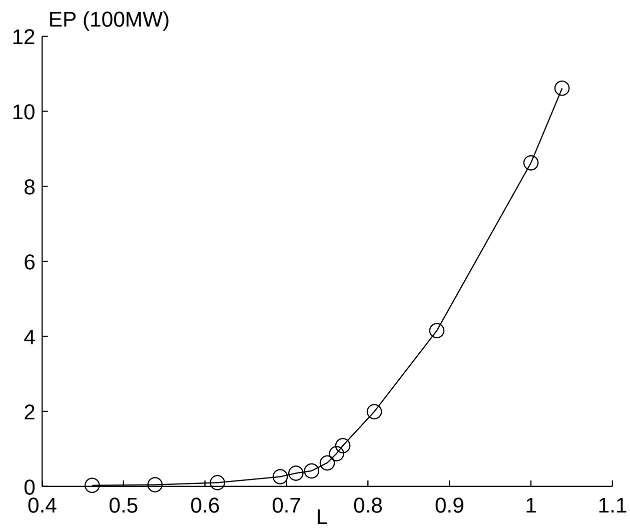

Figure 7. Variation of expected blackout size EP with loading L

To find out the probability distribution of blackout size P, binning of the data is used. Assume there are K sample points in bin j, and that each of the K points has the associated data pair $(P_i, \hat{\rho}_i)$. The representative $(\bar{P}_j, \bar{\hat{\rho}}_j)$ for bin j is defined as

$$\bar{P}_j = \frac{1}{K}\sum_{i=1}^{K} P_i \quad \text{and} \quad \bar{\hat{\rho}}_j = \frac{\sum_{i=1}^{K} P_i \hat{\rho}_i}{\bar{P}_j} \tag{13}$$

The variable binning used here is such that each bin starts with the minimum width and ends with at least a minimum number of samples.

Figures 8, 9, 10 show the pdf of blackout size P at the critical loading level 0.75, a higher level 0.85, and a lower level 0.62. The pdfs for loading levels 0.75 and 0.85 show some evidence of power tails. The 4 data points in Figure 9

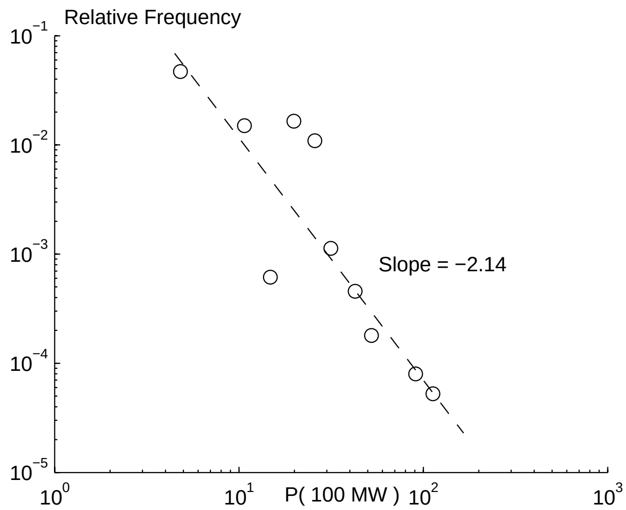

Figure 8. Distribution of blackout size P at loading $L = 0.75$

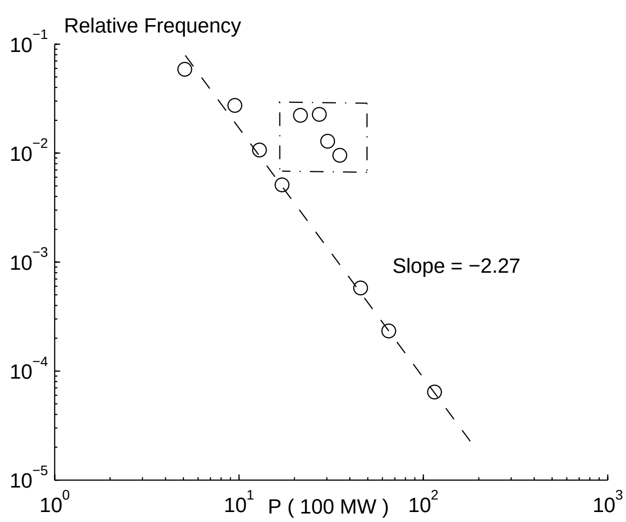

Figure 9. Distribution of blackout size P at loading $L = 0.85$

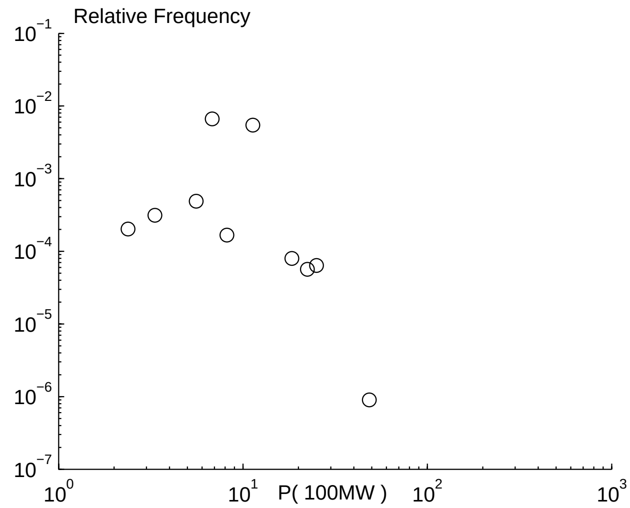

Figure 10. Distribution of blackout size P at loading $L = 0.62$

that lie well above the dotted line indicate a higher probability of medium size blackouts. This arises from artificial limitations on the further spread of blackouts of medium size, particularly the suppression of tripping in 45 negative impedance lines that represent highly equivalenced portions of network and in 60 lines that represent transformers (transformer failures are not modelled).

4. OPA model

The OPA model was developed to assess the possibility of self-organized criticality in series of electric power blackouts [10, 5, 7]. The self organization arises from the opposing forces of load growth and network upgrades in response to blackouts. In this paper we use a version of OPA with no load growth and a fixed network and it is this version which is summarized. For more detail see [10, 5, 7].

The OPA model represents transmission lines, loads and generators with the usual DC load flow assumptions. Starting from a solved base case, blackouts are initiated by a random line outage. Whenever a line is outaged, the generation and load is redispatched using standard linear programming methods. The cost function is weighted to ensure that load shedding is avoided where possible. If any lines were overloaded during the optimization, then these lines are outaged with probability p_1. The process of redispatch and testing for outages is iterated until there are no more outages. Thus OPA represents generic cascading outages which are consistent with basic network and operational constraints. A record is kept of the line overloads and outages and the load shed so that the blackout extent can be studied. $p_1 = 0$ ensures there are no line outages and only line overloads are considered whereas $p_1 = 1$ ensures that all overloaded lines outage.

We consider a fixed network with parameters chosen so that the system will be constrained by its transmission capacity as the load is increased. The network has 94 nodes, 12 generators and 82 loads arranged in a regular network with a tree-like form [6]. Most nodes have 3 incident transmission lines. A random fluctuation in loads is assumed up to a maximum of 20%. Blackout size is measured by the amount of load shed.

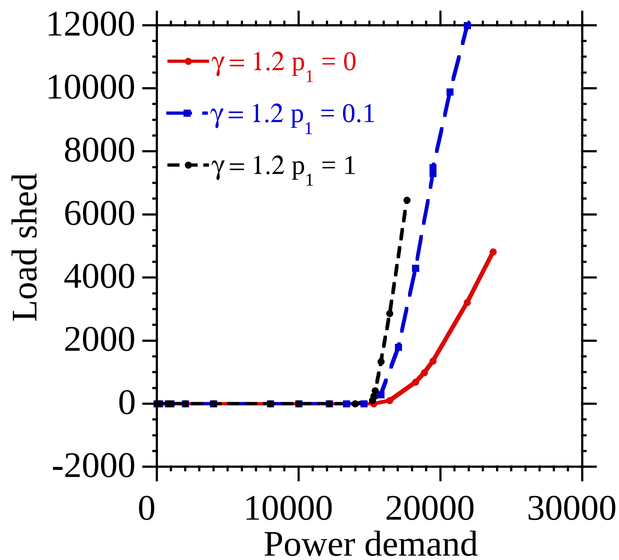

Figure 11. Mean blackout size versus loading.

Figure 11 shows mean blackout size as measured by the amount of load shed versus loading for three values of p_1. There is a critical loading $P = 15392$ at which the mean blackout size increases.

Figure 12 shows pdfs of blackout size as loading increases through the critical loading for $p_1 = 1$. The pdfs are shifted vertically so that their form may be seen.

At load $P = 15210$ (below the critical loading) the number of blackouts is small. The load fluctuations cause lines to overload and outage and hence some load shed. It common for a single line to outage so that only one load node is blacked out. This causes the pdf at lower blackout sizes to have a series of peaks associated with values of load at a single node.

At the critical loading $P = 15392$ there is some indication that a power tail develops with a decay index of about -1.5. The fall off after 0.08 is a network size effect. Above the critical loading the pdf is more Gaussian and is localized at a high value of the load shed.

The OPA model contains multiple critical points associ-

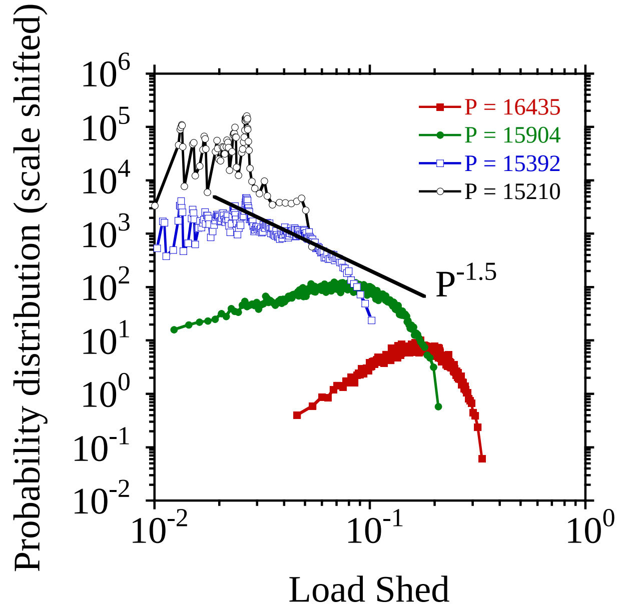

Figure 12. Distributions of blackout size.

ated with limits on both transmission and generation. In [7], we choose parameters so that the generation critical loading is reached first and scan through the critical loading by fixing the load and increasing the load fluctuations from zero to 98%. The results again show a power tail at the critical loading and a more exponential decay below and above the critical loading [7].

5. Discussion and Conclusions

We have examined expected blackout size and blackout size pdfs as load is increased in three different models: CASCADE, a hidden failure model, and the OPA model. All three models show a sharp increase in slope of the expected blackout size at a critical loading.

All three models show some evidence of power tails in the pdf at this critical loading, but there remain some differences and uncertainties in this result. In particular,

(1) CASCADE shows approximate power law behavior over a substantial range of blackout sizes near the critical loading. The CASCADE model is analytic so that the results are exact. CASCADE may represent processes occurring in cascading failure in power system but CASCADE is too simple to represent some presumably significant power system features.

(2) The hidden failure model shows power tails at and above the critical loading, except for some medium size blackouts. Below the critical loading the form of the pdf is not clear. This model represents hidden failures in the

protection system well and models power system cascading outages and overloads using the DC load flow approximation and LP redispatch. The results are obtained on a 179 bus equivalenced WSCC system.

(3) The OPA model shows some evidence of a power law region at critical loading and a more Gaussian form at higher or lower loadings. This model represents generic cascading power system outages and overloads using the DC load flow approximation and LP redispatch. The results are obtained on an artificial symmetric power system network of 96 nodes.

Since the three models are quite different and even the two simulation models are very approximate power system models, one cannot expect detailed agreement between the models or, for that matter, between the models and a real power system. (For example, [7] shows that the critical behavior of the OPA model is complicated and certainly cannot be reproduced in detail by CASCADE.) However, the broad agreement between the models is consistent with and supportive of the hypothesis that power tails in the pdf appear at a critical loading at which mean blackout size increases sharply. Moreover, it is possible that general features of cascading outages in power systems are captured by all three models; and in this case, the strengthened hypothesis is progress towards a global analysis and understanding of cascading failures in power systems. Further work testing the hypothesis to gain sharper conclusions is indicated.

Indeed, the hypothesis, if fully established, would have significant consequences for power system operation. For then the NERC blackout data [1, 5, 8] suggests that the North American power system has been operated near criticality. Moreover, it is then plausible that the power tails and the consequent risk of large blackouts could be substantially reduced by lowering power system loading to obtain an exponential tail for large blackouts. It would be better to analyze this tradeoff between catastrophic blackout risk and loading instead of just waiting for the effects to manifest themselves in the North American power system!

Why would power systems be operated near a critical loading? One possible answer is that overall forces, including the system engineering and operational policies, organize the system towards criticality as proposed in [4, 5, 10, 6, 7].

A notable outcome of this paper is the CASCADE model and the derivation of formulas for its pdf. This pdf exhibits heavy tails near critical loading and more exponential tails far from critical loading (high loading also yields a significant chance of total failure). This is a new model of probabilistic cascading failure that is of general interest in studying the distribution of sizes of failures of large interconnected systems in which the successive failure of loaded components progressively weakens the system.

6. Acknowledgements

I. Dobson, J.S. Thorp, J. Chen, and B.A. Carreras gratefully acknowledge coordination of this work by the Consortium for Electric Reliability Technology Solutions and funding in part by the Assistant Secretary for Energy Efficiency and Renewable Energy, Office of Power Technologies, Transmission Reliability Program of the U.S. Department of Energy under contract 9908935 and Interagency Agreement DE-A1099EE35075 with the National Science Foundation. I. Dobson and D.E. Newman gratefully acknowledge support in part from National Science Foundation grants ECS-0085711 and ECS-0085647. Part of this research has been carried out at Oak Ridge National Laboratory, managed by UT-Battelle, LLC, for the U.S. Department of Energy under contract number DE-AC05-00OR22725. I. Dobson thanks H-D. Chiang and the School of ECE at Cornell University for their generous hospitality during a sabbatical leave.

References

[1] Information on electric systems disturbances in North America can be downloaded from the NERC website at http://www.nerc.com/dawg/database.html

[2] K. Bae, J.S. Thorp, A stochastic study of hidden failures in power system protection, Decision Support Systems, vol. 24, pp. 259-268, 1999.

[3] J.A. Bucklew, Large deviation techniques in decision, simulation, and estimation, Wiley 1990.

[4] B.A. Carreras, D.E. Newman, I. Dobson, A.B. Poole, Initial evidence for self-organized criticality in electric power system blackouts, 33rd Hawaii International Conference on System Sciences, Maui, Hawaii, January 2000.

[5] B.A. Carreras, D.E. Newman, I. Dobson, A.B. Poole, Evidence for self-organized criticality in electric power system blackouts, 34th Hawaii International Conference on System Sciences, Maui, Hawaii, January 2001.

[6] B.A. Carreras, V.E. Lynch, M. L. Sachtjen, I. Dobson, D.E. Newman, Modeling blackout dynamics in power transmission networks with simple structure, 34th Hawaii International Conference on System Sciences, Maui, Hawaii, January 2001.

[7] B.A. Carreras, V.E. Lynch, I. Dobson, D.E. Newman, Dynamics, criticality and self-organization in a model for blackouts in power transmission systems, 35th Hawaii International Conference on System Sciences, Hawaii, January 2002.

[8] J. Chen, J.S. Thorp, M. Parashar, Analysis of electric power disturbance data, 34th Hawaii International Conference on System Sciences, Maui, Hawaii, January 2001.

[9] P.C. Consul, A simple urn model dependent upon predetermined strategy, Sankhyā: The Indian Journal of Statistics, Series B, vol. 36, Pt. 4, 1974, pp. 391-399.

[10] I. Dobson, B.A. Carreras, V. Lynch, D.E. Newman, An initial model for complex dynamics in electric power system blackouts, 34th Hawaii International Conference on System Sciences, Maui, Hawaii, January 2001.

[11] J.S. Thorp, A.G. Phadke, et al., Anatomy of power system disturbances: Importance sampling, Power System Computation Conference, Dresden, Aug. 1996.

[12] A.J. Wood, B.F. Wollenberg, Power system generation, operation and control, Wiley 1984.

A. Derivation of CASCADE distribution

It is convenient to to work in terms of line margins $M_1, M_2, M_3, \cdots, M_n$ where $M_j = 1 - L_j$. Then $M_1, M_2, M_3, \cdots, M_n$ are independent random variables uniform on $[0, 1 - L^{min}]$. Recall that the integer $q = (1 - L^{min})/\Delta = 1/p$.

We suppose that $r \leq q - 1$ and examine the event $[S = r]$, which is a cascade of exactly r lines. Suppose we renumber the lines so that the r lines outaged in the order $1, 2, ..., r$. The initial disturbance increased the loading on line 1 by Δ. Since line 1 outaged, its margin M_1 must have been less than Δ. The outage of line 1 caused an additional increase of loading Δ on all the lines. Since line 2 outaged, its margin M_2 must have been less than 2Δ. Similarly, for $j \leq r$, since line j outaged, its margin M_j must have been less than $j\Delta$. After line r outages, the remaining intact lines all have had their loadings increased by $(r+1)\Delta$. ($(r+1)\Delta$ comprises the initial disturbance Δ and Δ for each of the r lines outaged.) Since none of the remaining intact lines outaged, their margins must all exceed or equal $(r + 1)\Delta$. To summarize:

$$M_1 < \Delta, M_2 < 2\Delta, \cdots, M_r < r\Delta,$$
$$M_k \geq (r + 1)\Delta \qquad \text{for } r + 1 \leq k \leq n.$$

The same argument without renumbering the lines and accounting for the possible permutations of lines yields

$$[S = r] = \bigcup_{\pi \in S_n} [M_{\pi(1)} < \Delta, M_{\pi(2)} < 2\Delta, \cdots, M_{\pi(r)} < r\Delta, M_{\pi(r+1)} \geq (r + 1)\Delta, \cdots, M_{\pi(n)} \geq (r + 1)\Delta] \quad (14)$$

where the union runs over all permutations π of $1, 2, \cdots, n$ in the symmetric group S_n. The union in (14) is not a disjoint union.

We consider the case $r > q - 1$. If the cascade extends to a size $r > q - 1$, then the total increase in load on the remaining intact lines is $(r+1)\Delta > q\Delta = 1 - L^{min}$. Since $1 - L^{min}$ is the maximum line margin, all the remaining intact lines must outage, and so $S = n$ and $P[S = r] = 0$ for $q - 1 < r < n$.

In the case $r = q - 1$, (14) applies but, since $(r + 1)\Delta = q\Delta = 1 - L^{min}$, the event $[M_{\pi(n)} \geq (r + 1)\Delta]$ becomes the probability zero event $[M_{\pi(n)} = 1 - L^{min}]$ and hence $P[S = q - 1] = 0$.

Now we assume $r < q - 1$ for the rest of this appendix. Define intervals $I_1, I_2, \cdots, I_q$ so that

$$I_j = [(j - 1)\Delta, j\Delta) \quad ; 1 \leq j \leq q \quad (15)$$

Then
$$[M_{\pi(\ell)} < \ell\Delta] = \bigcup_{a_\ell \in \{1,2,\ldots,\ell\}} [M_{\pi(\ell)} \in I_{a_\ell}]$$
$$[M_{\pi(\ell)} \geq (r + 1)\Delta] = \bigcup_{a_\ell \in \{r+2,\ldots,q\}} [M_{\pi(\ell)} \in I_{a_\ell}]$$

and (14) can be written as

$$[S = r] = \bigcup_{\pi \in S_n} \bigcup_{(a_1,a_2,\ldots,a_n) \in B} [M_{\pi(1)} \in I_{a_1}, M_{\pi(2)} \in I_{a_2}, \cdots, M_{\pi(n)} \in I_{a_n}] \quad (16)$$

where $B = \{(a_1, a_2, ..., a_n) \mid a_1 \in \{1\}, a_2 \in \{1, 2\}, ..., a_r \in \{1, 2, ..., r\}, a_{r+1} \in \{r + 2, ..., q\}, ..., a_n \in \{r + 2, ..., q\}\}$

In (16) it is equivalent to permute the intervals I_{a_i} instead of permuting the margins M_i:

$$[S = r] = \bigcup_{\pi \in S_n} \bigcup_{(a_1,a_2,\ldots,a_n) \in B} [M_1 \in I_{a_{\pi(1)}}, M_2 \in I_{a_{\pi(2)}}, \cdots, M_n \in I_{a_{\pi(n)}}] \quad (17)$$

and (17) may be rewritten as

$$[S = r] = \bigcup_{(a_1,a_2,\ldots,a_n) \in B_\pi} [M_1 \in I_{a_1}, M_2 \in I_{a_2}, \cdots, M_n \in I_{a_n}] \quad (18)$$

where B_π is the set of permuted elements of B:

$$B_\pi = \bigcup_{\pi \in S_n} \{(a_{\pi(1)}, a_{\pi(2)}, ..., a_{\pi(n)}) \mid a_1 \in \{1\}, a_2 \in \{1, 2\}, ..., a_r \in \{1, 2, ..., r\}, a_{r+1} \in \{r + 2, ..., q\}, ..., a_n \in \{r + 2, ..., q\}\} \quad (19)$$

For each i with $1 \leq i \leq n$, the event $[M_i \in I_{a_i}]$ has probability p. Since $M_1, M_2, \cdots, M_n$ are independent, the event $[M_1 \in I_{a_1}, M_2 \in I_{a_2}, \cdots, M_n \in I_{a_n}]$ has probability p^n. Equation (18) expresses $[S = r]$ as a disjoint union of events $[M_1 \in I_{a_1}, M_2 \in I_{a_2}, \cdots, M_n \in I_{a_n}]$. Therefore, writing $|B_\pi|$ for the number of elements of B_π,

$$P[S = r] = |B_\pi|\, p^n \quad (20)$$

and the computation of $P[S = r]$ reduces to counting the number of elements of B_π.

$$\text{Define} \quad A_r = \bigcup_{\pi \in S_r} \{(a_{\pi(1)}, a_{\pi(2)}, ..., a_{\pi(r)}) \mid a_1 \in \{1\}, a_2 \in \{1,2\}, ..., a_r \in \{1,2,...,r\}\} \quad (21)$$

$$A'_r = \bigcup_{\pi \in S_{n-r}} \{(a_{\pi(1)}, a_{\pi(2)}, ..., a_{\pi(n-r)}) \mid a_1 \in \{r+2,...,q\}, ..., a_{n-r} \in \{r+2,...,q\}]$$

Each element of B_π can be uniquely specified by first choosing which $n-r$ of $\{a_1, a_2, ..., a_n\}$ are in $\{r+2, ..., q\}$, or, equivalently, which r of $\{a_1, a_2, ..., a_n\}$ are less than $r+1$, and then making a choice of one element of A_r, and then making a choice of one element of A'_r. Therefore

$$|B_\pi| = \binom{n}{n-r} |A_r||A'_r| = \binom{n}{r} |A_r||A'_r| \quad (22)$$

It is straightforward that $|A'_r| = (q-(r+1))^{n-r}$ and Lemma 1 below yields $|A_r| = (r+1)^{r-1}$. Hence

$$|B_\pi| = \binom{n}{r} (r+1)^{r-1}(q-(r+1))^{n-r} \quad (23)$$

It follows from (20), (23) and $pq = 1$ that

$$P[S = r] = \frac{1}{r+1} \binom{n}{r} ((r+1)p)^r (1-(r+1)p)^{n-r} \quad (24)$$

Lemma 1 *Define the set* A_r *by* (21). *Then*

$$|A_r| = (r+1)^{r-1} \quad (25)$$

Proof: Define

$$\Sigma_{r+1} = \{(a_1, a_2, ..., a_r) \mid a_i \in \{1,2,...,r+1\},\ i = 1,2,...,r\} \quad (26)$$

Then $A_r \subset \Sigma_{r+1}$ and $|\Sigma_{r+1}| = (r+1)^r$.

Define the permutation σ_1 on $\{1,2,...,r+1\}$ by

$$\sigma_1(a) = \begin{cases} a+1 & ; 1 \le a \le r \\ 1 & ; a = r+1 \end{cases} \quad (27)$$

Define $\sigma : \Sigma_{r+1} \to \Sigma_{r+1}$ by

$$\sigma((a_1, a_2, ..., a_r)) = (\sigma_1(a_1), \sigma_1(a_2), ..., \sigma_1(a_r)) \quad (28)$$

σ^{r+1} is the identity and $\{1, \sigma, \sigma^2, ..., \sigma^r\}$ is a cyclic group acting on Σ_{r+1}.

Consider the following union of subsets of Σ_{r+1}:

$$A_r \cup \sigma(A_r) \cup \sigma^2(A_r) \cup \cdots \cup \sigma^r(A_r) \quad (29)$$

To prove the Lemma it is sufficient to show that (29) is a partition of Σ_{r+1} into $r+1$ sets of equal size. For then $(r+1)|A_r| = |\Sigma_{r+1}| = (r+1)^r$.

The equal size of $A_r, \sigma(A_r), \sigma^2(A_r), \cdots, \sigma^r(A_r)$ follows from σ being a bijection. To prove that (29) is a partition, we need $A_r, \sigma(A_r), \sigma^2(A_r), \cdots, \sigma^r(A_r)$ to be disjoint and that (29) is equal to Σ_{r+1}.

Let k satisfy $1 \le k \le r$.

$$\sigma^k(A_r) = \bigcup_{\pi \in S_r} \{(a_{\pi(1)}, a_{\pi(2)}, ..., a_{\pi(r)}) \mid a_1 \in \{k+1\}, a_2 \in \{k+1, k+2\}, \cdots, a_{r+1-k} \in \{k+1, ..., r+1\}, a_{r+2-k} \in \{k+1, ..., r+1, 1\}, a_{r+3-k} \in \{k+1, ..., r+1, 1, 2\}, \cdots, a_r \in \{k+1, ..., r+1, 1, 2, ..., k-1\}\} \quad (30)$$

By inspection of (21) and (30), each element of A_r has at least k entries from $\{1,2,...,k\}$ and each element of $\sigma^k(A_r)$ has no more than $k-1$ entries from $\{1,2,...,k\}$. Therefore A_r and $\sigma^k(A_r)$ are disjoint for $1 \le k \le r$. Then $A_r, \sigma(A_r), \sigma^2(A_r), \cdots, \sigma^r(A_r)$ are disjoint, for if not, then there are m, ℓ with $0 \le m < \ell \le r$ and $1 \le \ell - m \le r$ and there is a $b \in \sigma^m(A_r) \cap \sigma^\ell(A_r)$ and $\sigma^{-m}(b) \in A_r \cap \sigma^{\ell-m}(A_r)$, which is a contradiction.

To show that the subset (29) of Σ_{r+1} is equal to Σ_{r+1}, we choose any $b = (b_1, b_2, ..., b_r) \in \Sigma_{r+1}$ and show that b is in (29). Define $|b| = |(b_1, b_2, ..., b_r)| = b_1 + b_2 + ... + b_r$. Choose k which minimizes $|\sigma^k(b)|$ and write $c = (c_1, c_2, ..., c_r) = \sigma^k(b)$.

We now show that $c \in A_r$. Since A_r contains all permutations of its elements, we can reorder $(c_1, c_2, ..., c_r)$ without loss of generality so that $c_1 \le c_2 \le ... \le c_r$. According to (21), $c_i \in \{1,2,...,i\}$, $i = 1,2,...,r$ implies $c \in A_r$. We prove $c_i \in \{1,2,...,i\}$, $i = 1,2,...,r$ by induction on i.

$c_1 \in \{1\}$, for if $c_1 > 1$, then $c_j \ge 2$ for $j = 1,2,...,r$ and $\sigma_1^{-1}(c_j) = c_j - 1$ for $j = 1,2,...,r$ and $|\sigma^{-1}(c)| = |c| - r < |c|$ which is a contradiction.

Now suppose that i satisfies $2 \le i \le r$ and that $c_\ell \in \{1,2,...,\ell\}$ for $\ell < i$. Then $\sigma_1^{-i}(c_j) = c_j + r + 1 - i$ for $j = 1,2,...,i-1$. Suppose that $c_i \notin \{1,2,...,i\}$. Then $c_j \ge i+1$ for $j = i, i+1, ..., r$ and $\sigma_1^{-i}(c_j) = c_j - i$ for $j = i, i+1, ..., r$. Now $|\sigma^{-i}(c)| = |c| + (i-1)(r+1-i) - (r+1-i)i = |c| - (r+1-i) < |c|$ which is a contradiction. Therefore $c_i \in \{1,2,...,i\}$.

Thus $c \in A_r$. It follows that $b = \sigma^{-k}(c) = \sigma^{r+1-k}(c) \in \sigma^{r+1-k}(A_r)$ is in (29).